Supporting Information for "Quantifying the interplay of Meltwater and Ice-Albedo Feedbacks in the Arctic Ice-Ocean System"

Haohao Zhang[1, 2, 3], Andrea Storto[2], Xuezhi Bai[1, 3] and Chunxue Yang[2]

[1]College of Oceanography, Hohai University, Nanjing 210024, China.
[2]Institute of Marine Sciences (ISMAR), National Research Council (CNR), Rome, Italy.
[3]Key Laboratory of Marine Hazards Forecasting, Ministry of Natural Resources, Hohai University, Nanjing 210024, China.

Correspondence to: Xuezhi Bai (xuezhi.bai@hhu.edu.cn)

Contents of this file

1 Model Validation

1.1 Validation of Background mixing coefficient

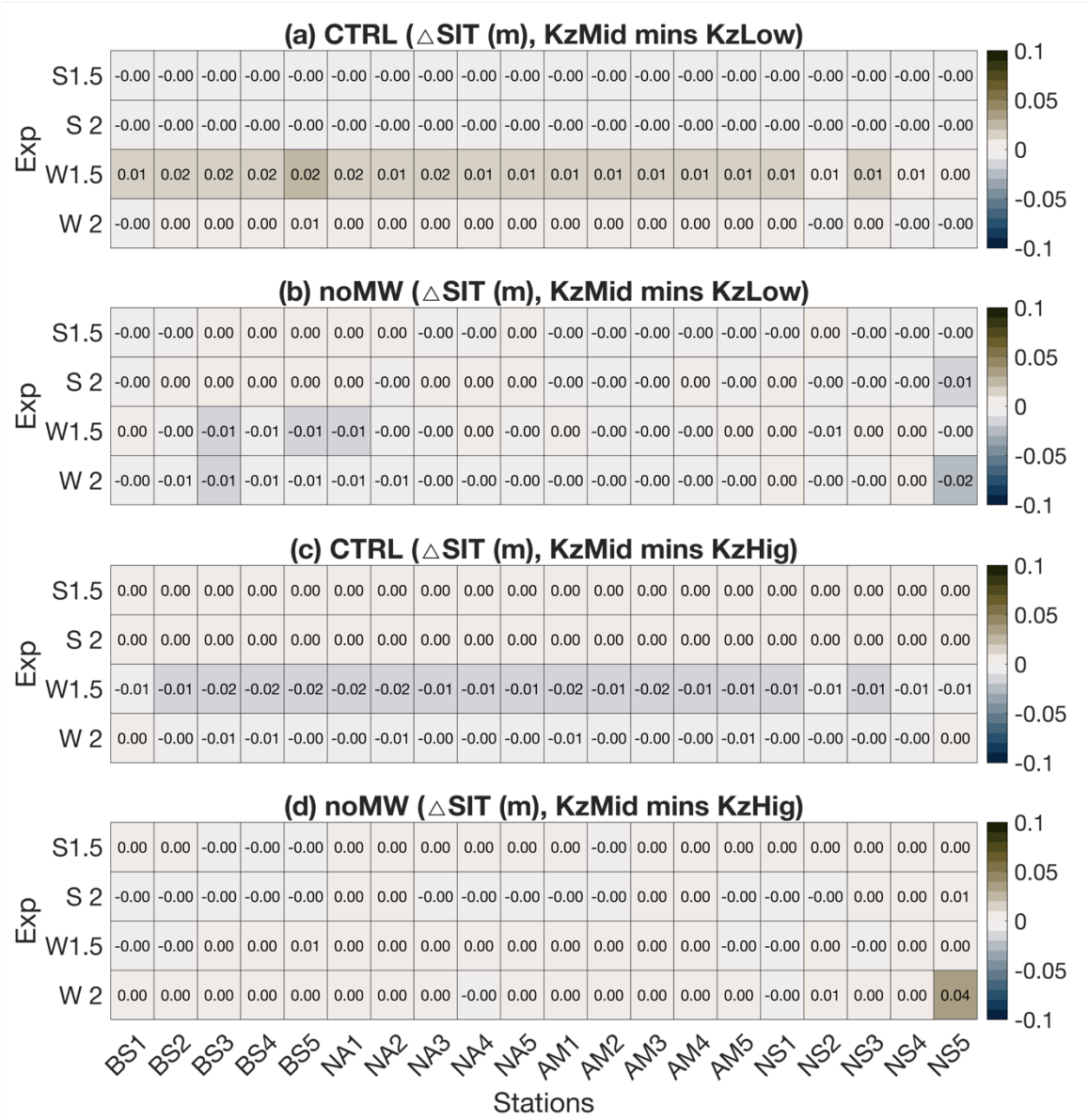

Figure S1. Heatmap of simulated sea ice thickness (SIT) difference at all stations for three background mixing parameters. In the title KzLow= $10^{-7}\ m^2 s^{-1}$; KzMid= $5.44 \times 10^{-7}\ m^2 s^{-1}$; KzHig= $10^{-6}\ m^2 s^{-1}$. The y-axis labels 'S1.5' and 'S2' indicate the summer sea ice melting thickness for experiments with initial SIT of 1.5 m and 2 m, respectively, and 'W1.5' and 'W2' indicate the winter ice freezing thickness for experiments with initial SIT of 1.5m and 2 m.

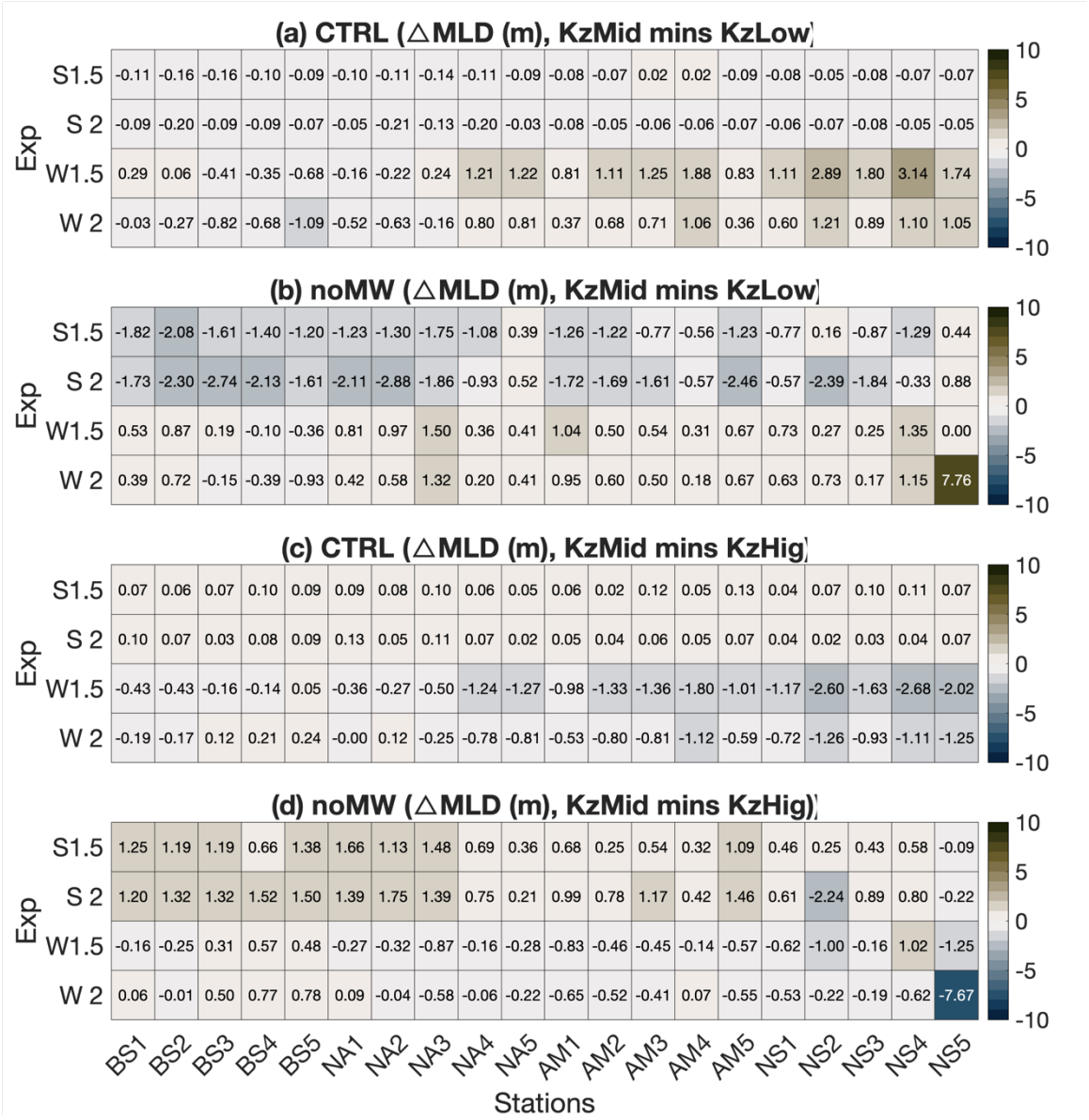

40 **Figure S2. Same as Figure S1 but for mixed layer depth (MLD).**

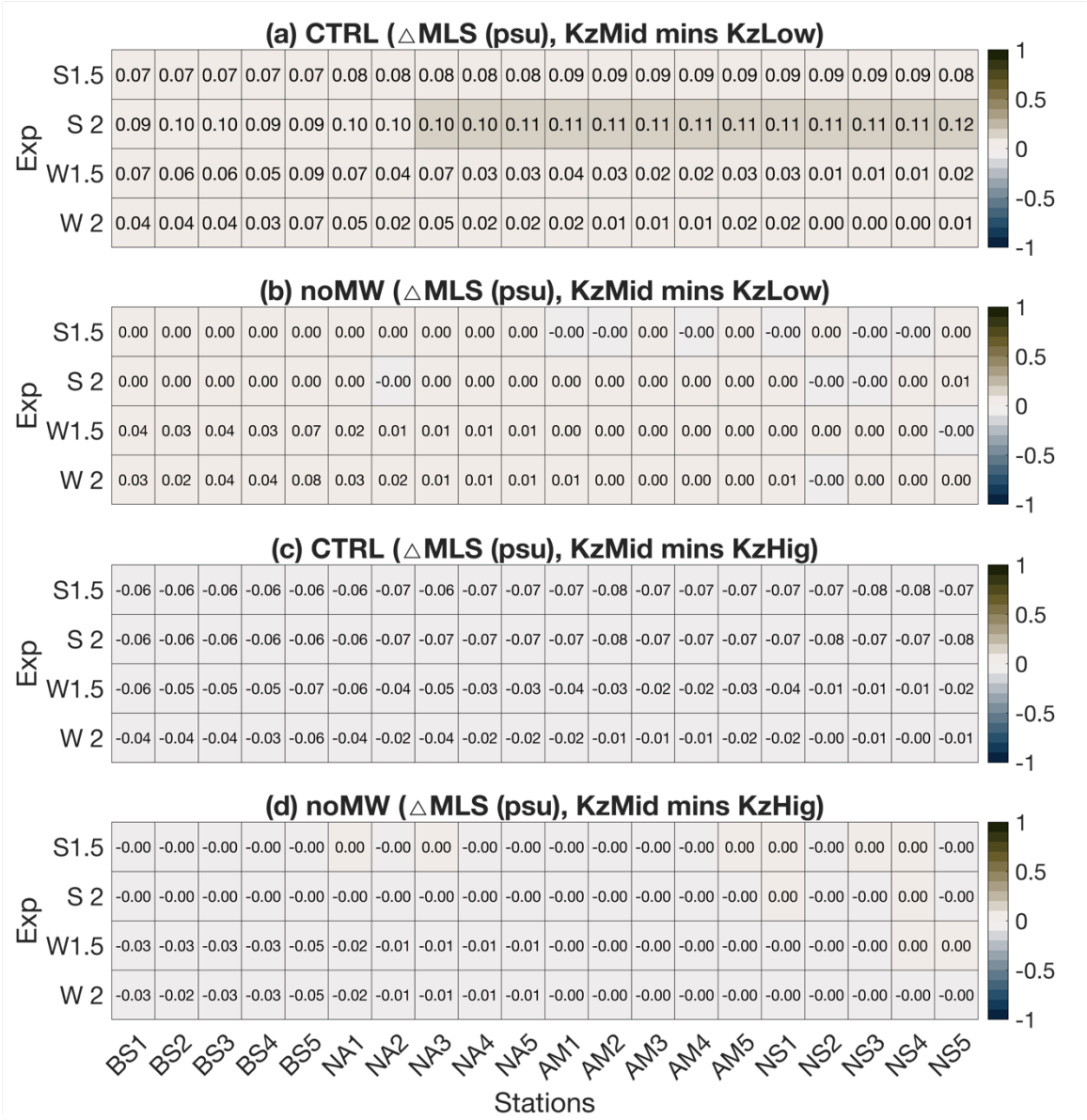

Figure S3. Same as Figure S1 but for mixed layer salinity (MLS).

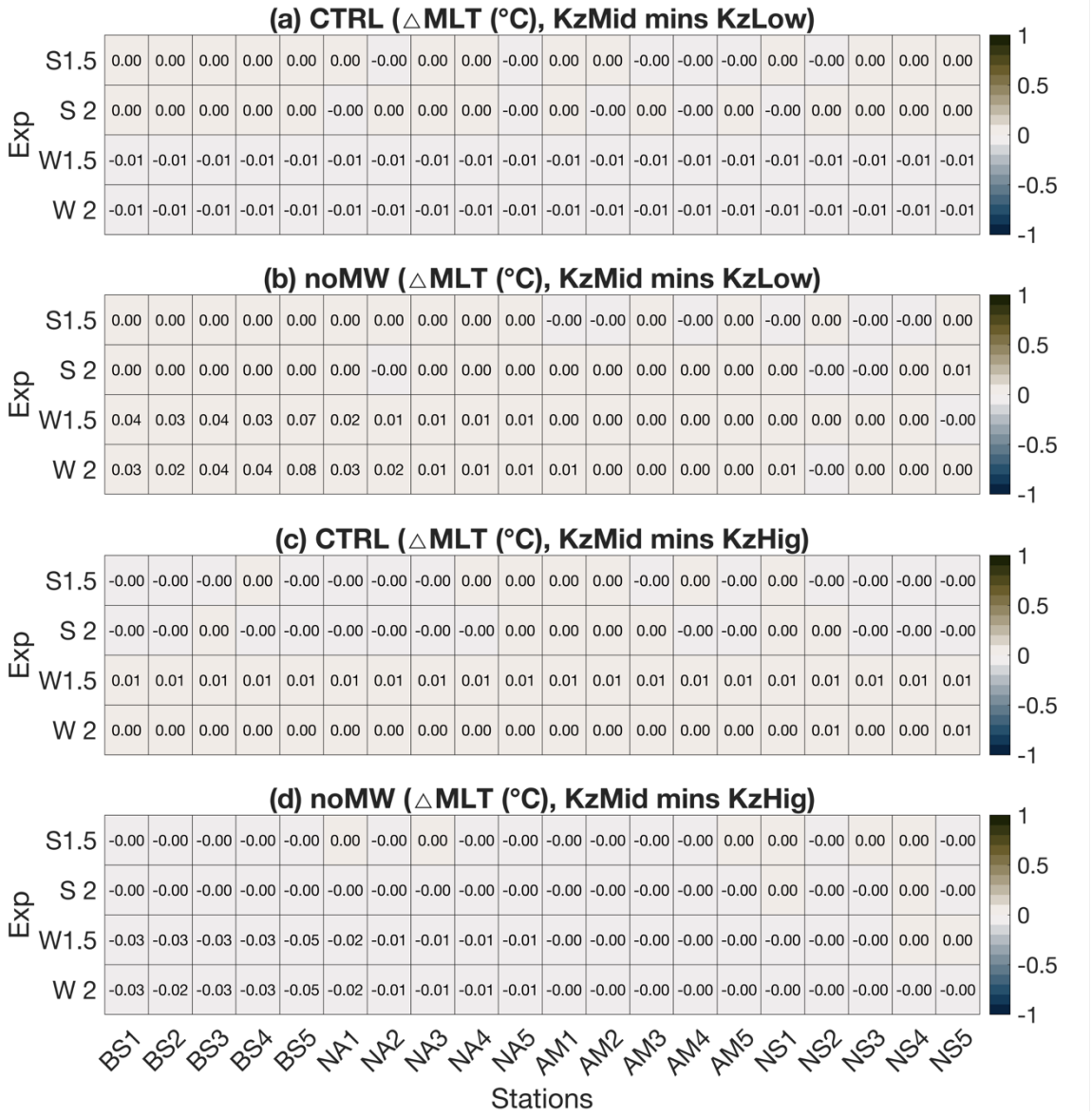

Figure S4. Same as Figure S1 but for mixed layer temperature (MLT).

1.2 Validation of boundary conditions at the bottom

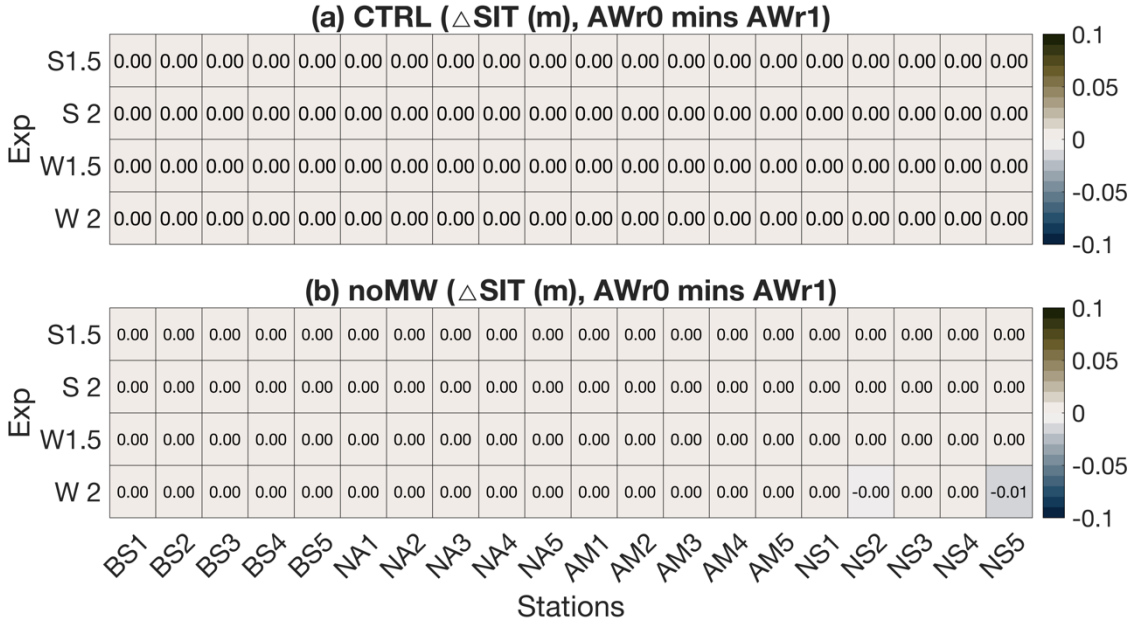

Figure S5. Heatmap of simulated sea ice thickness (SIT) difference at all stations between two boundary conditions in the CTRL run and MW0 run. AWr0 means no bottom boundary conditions and AWr1 means with a 1-day recovery period in the bottom. The y-axis labels 'S1.5' and 'S2' indicate the summer sea ice melting thickness for experiments with initial SIT of '1.5m' and '2m', respectively, and 'W1.5' and 'W2' indicate the winter ice freezing thickness for experiments with initial SIT of '1.5m' and '2m'.

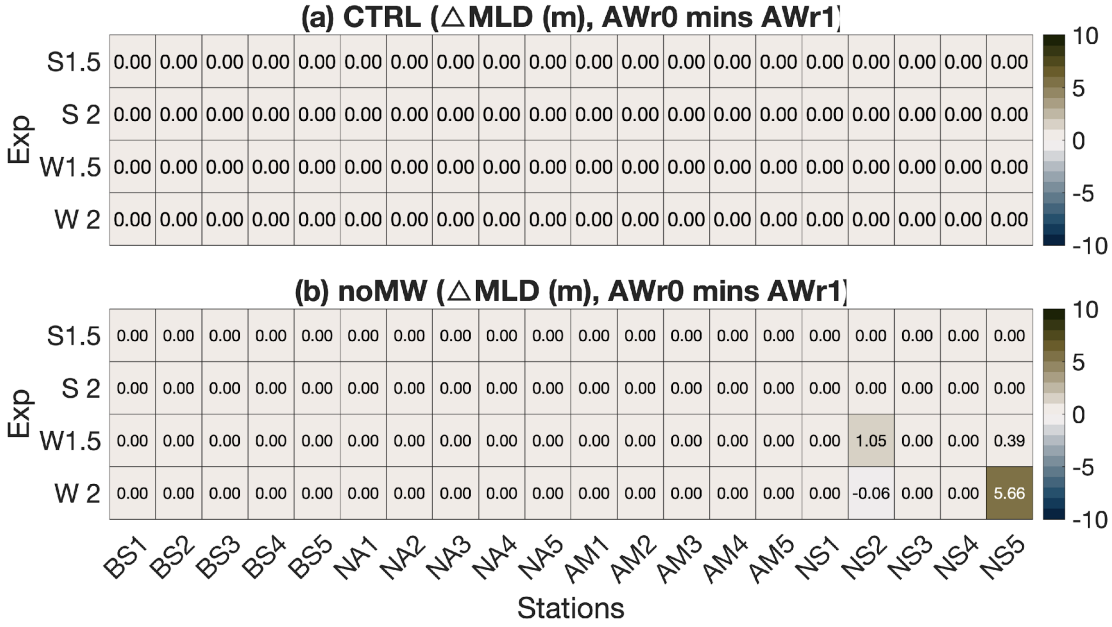

Figure S6. Same as Figure S5 but for MLD.

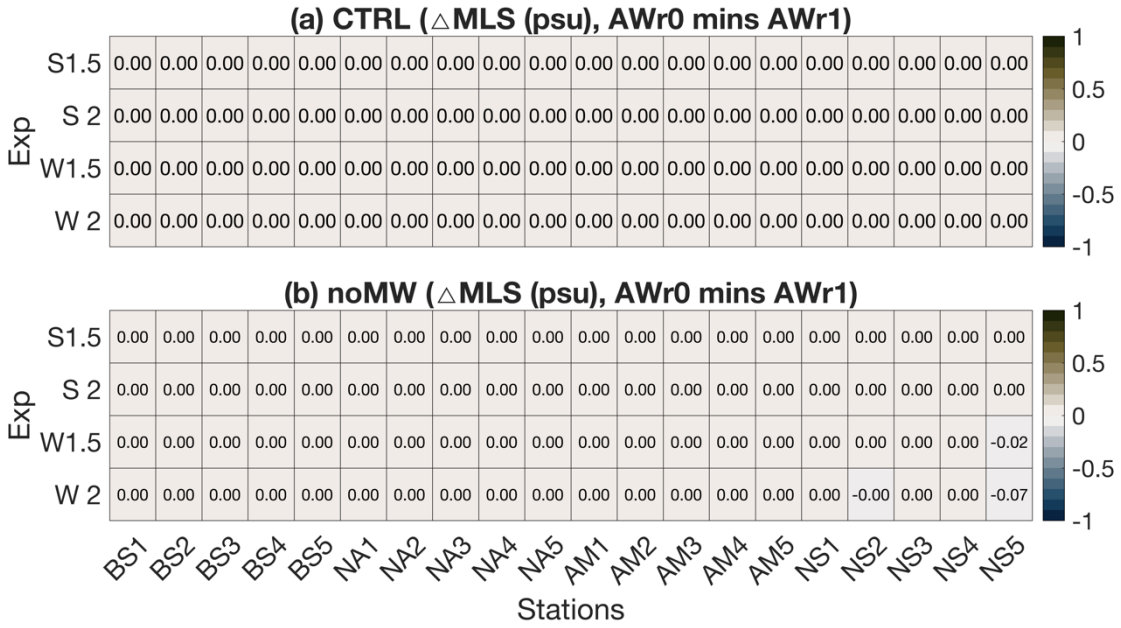

Figure S7. Same as Figure S5 but for MLS.

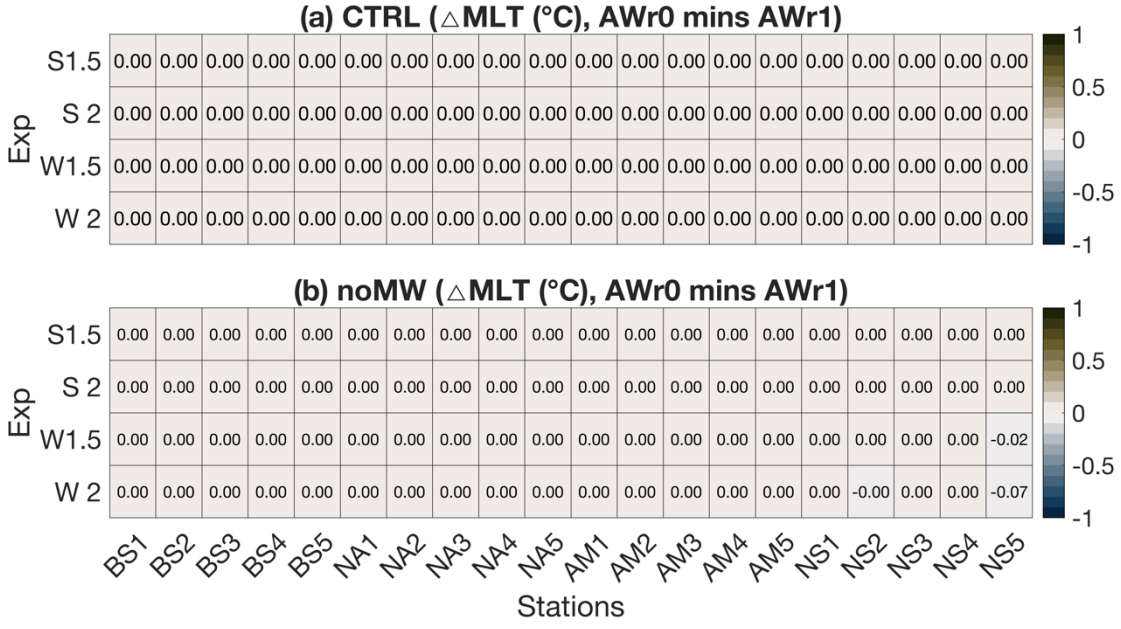

Figure S8. Same as Figure S5 but for MLT.

1.3 Runoff forcing

In order to verify the choice of 1200 km^3 is reasonable, we conducted experiments using freshwater forcing values of 6400 km^3 (Runoff plus P-E, as described in Section 1 in the main text) and 1200 km^3(net Arctic freshwater input), respectively. The results show that a forcing value of 6400 km^3 causes excessive freshwater accumulation at the surface, resulting in a maximum mixed layer depth (MLD) of only ~ 25 m in winter across all regions (Fig. S5, red lines). This is clearly unreasonable compared to observed values, which shows the MLD in the Canadian Basin is approximately 30 m, and in the Eurasian Basin, it ranges from about 70 to over 100 m during winter (Peralta-Ferriz and Woodgate, 2015). In contrast, the experimental results using a freshwater forcing of 1200 km³/y are much more reasonable and closer to the observations. (Fig. S5, blue lines).

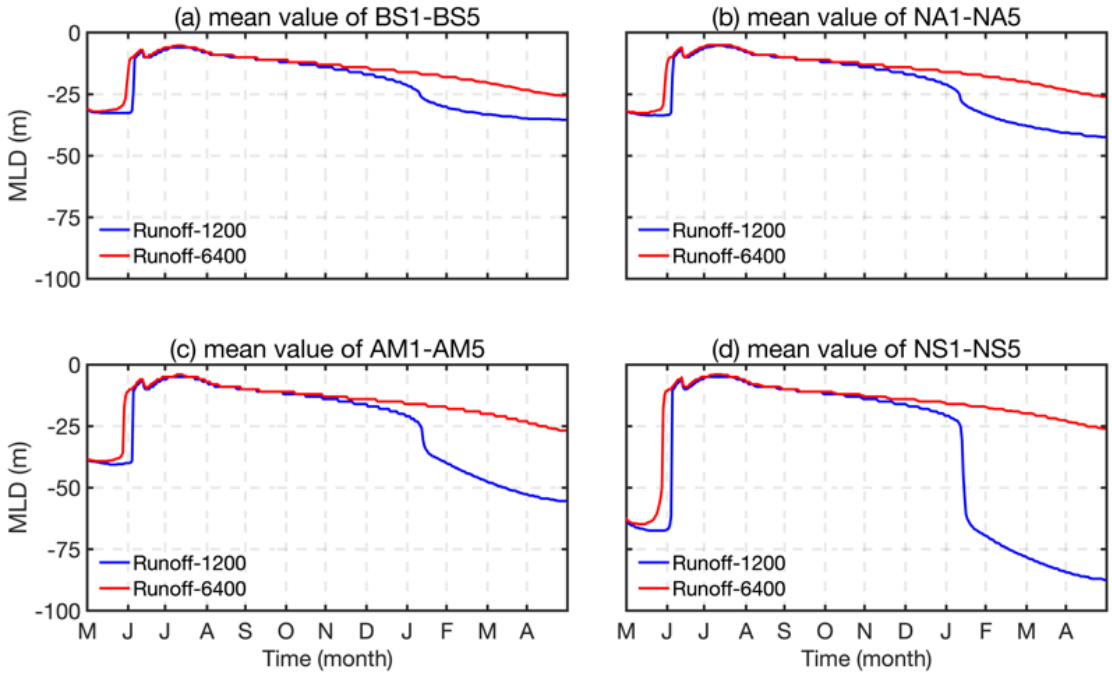

Figure S9. Time series of the mean MLD for each basin, obtained from simulations using runoff forcing values of 1200 km³ (blue lines) and 6400 km³ (red lines). (a): Beaufort Sea (BS); (b): Northern Americana Basin (NA); (c): Amundsen Basin (AM); (d): Nansen Basin (NS).

1.4 Comparison with observations

In the CTRL run, the simulated average minimum summer sea ice thickness across all 20 stations is 0.91 ± 0.04 m, which closely matching the observed value of 0.82 ± 0.11 m in the Arctic Ocean at the end of the melting season during 2011-2020 (Landy et al., 2022). This indicates that the sea ice results from our 1D model align well with actual Arctic sea ice conditions.

The 1D model used in this study also reproduces the seasonal changes in the vertical structure of the Arctic Ocean well. The MLD changes of the Arctic Ocean are significantly influenced by the annual cycle of sea ice melting and formation, showing strong seasonal variations of deeper in winter and shallower in summer (such as Fig. 4m and q in the main text). Statistical analysis of various hydrographic profile observations shows that the MLDs during July and August are 8.7 ± 3.6 m in the Canadian Basin and 22 ± 13 m in the Eurasian Basin, calculated using the threshold criterion of σ=0.03 kg m^{-3} (Peralta-Ferriz and Woodgate, 2015). The model results show similar summer mixed layer depth (MLD) values across stations under the same threshold criterion and month time, with an average summer MLD of ~7.6 m in the CTRL runs, which means the simulated values in the Canadian Basin closely match the observations, while those in the Eurasian Basin are relatively shallow. In the Eurasian Basin, the inflow of highly saline Atlantic water drives interactions between the seasonal mixed layer (ML) and the ocean interior (Carmack et al., 2016; Polyakov et al., 2017). Because this 1D model simulations exclude advection flux processes and the Eurasian Basin is more saline, the surface layer is more susceptible to a larger salinity gradient due to the lack of advection-replenished saline water and the continuous release of freshwater from ice melting, which may contribute to the modeled shallower summer MLD. In winter, the observed April MLDs are approximately 33 ± 8 m in the Canadian Basin and ~70 to 100+ m in the Eurasian Basin. Our simulations show that the average MLD in April is ~35 m for all CTRL runs in the Canadian Basin and ~70 m in the Eurasian Basin. In particular, the MLD can exceed 100 m in April at stations NS2 and NS4. Our model also accurately reproduces the appearance and changes of the NSTM (such as Fig. 4q in the main text), which is the remnant solar heat trapped beneath the ML and a notable feature in the Canadian Basin, caused by penetrative shortwave solar heating principally through leads (Jackson et al., 2010; Maykut and McPhee, 1995; Steele et al., 2011). In addition, the ITP41 captured NSTM changes very well and had short spatial drift between May 2011 and April 2012. We further validated the model by simulating the ITP41 case with its corresponding atmospheric forcing field and initial conditions, and the results show the model's capability to replicate the observed seasonal thermohaline variations (Fig. S10). Based on the observations, the ocean-ice heat flux (F_{oi}) has a significant seasonal cycle with maximum values reaching 40-60 W/m2 in summer (Maykut & McPhee, 1995) and close to zero during winter in many instances (Krishfield & Perovich, 2005; McPhee et al., 2003; Zhong et al., 2022). The model results of the CTRL agree with the observed values well (e.g., FigureS14a and b, black lines and Figure8 in main text).

In conclusion, our 1D model simulated summer ice condition and seasonal variations in the vertical structure of the Arctic Ocean in qualitative agreement with observations. While the CTRL run does not aim to precisely replicate observed values, it provides a baseline of reasonable accuracy for comparing differences between CTRL and sensitivity experiments.

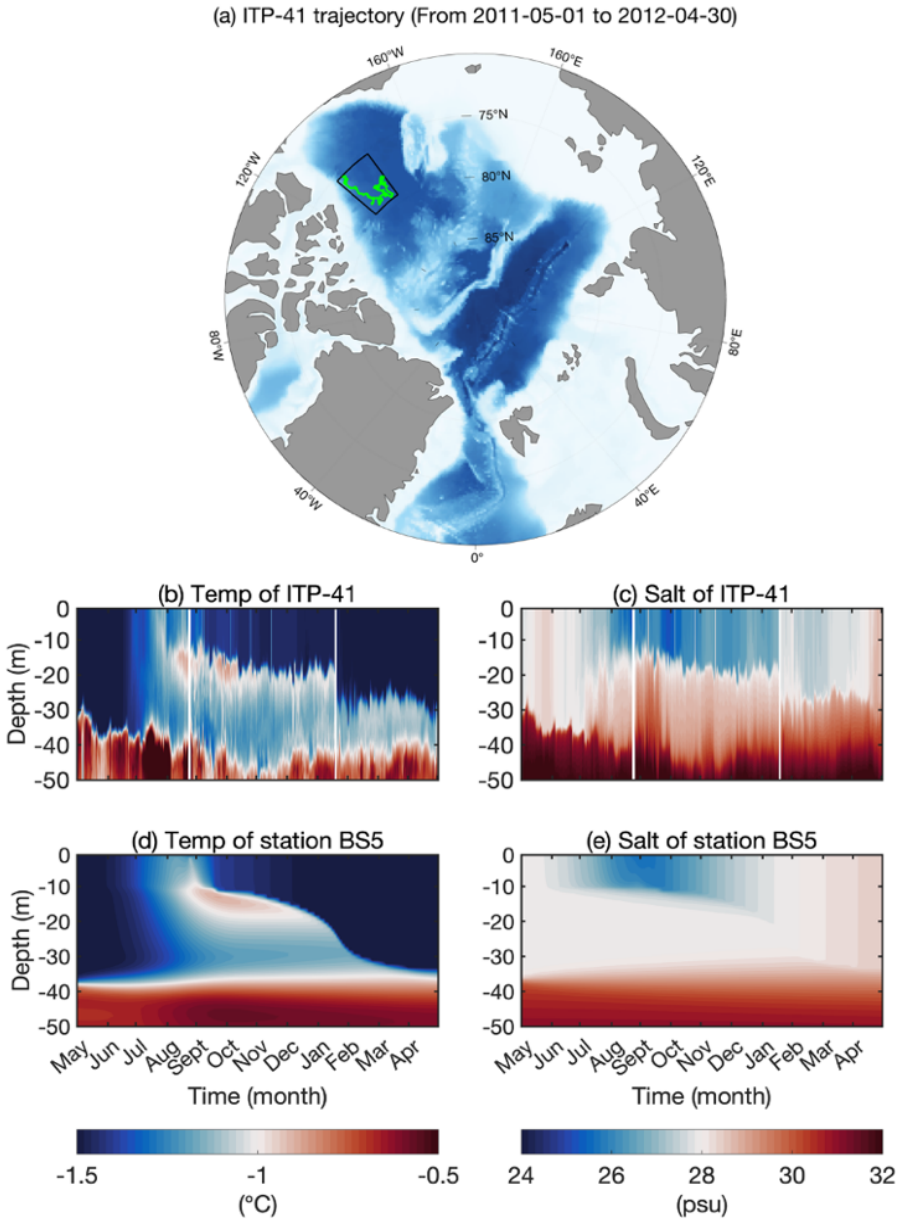

Figure S10. (a) Trajectory of ITP 41 from May 2011 to April 2012 shown in green. In this case simulation, the atmospheric forcing field is derived from NCEP-DOE (https://psl.noaa.gov) and averaged over the region outlined by the black line, covering the same time as ITP 41. Initial ice and snow thicknesses are taken from NSIDC (https://nsidc.org/data/nsidc-0773/versions/1) regional averages for May 2011. (b)–(e): Time series of temperature (left column) and salinity (right column) in the upper 50 m, derived from (b, c) ITP 41 observations and (d, e) simulation results.

2 Model results for experiments with initial SIT of 1.5 m

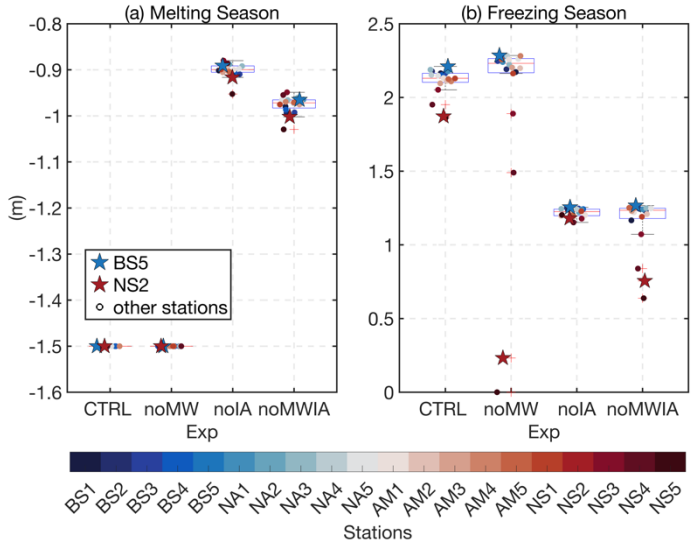

Figure S11. Box plots illustrating the (a) ice thickness changes during the melting season and (b) freezing season across different Stations in different types of experiments. Different stations are indicated by different colored dots. Each box plot shows the median, interquartile range, and potential outliers (points marked with red plus sign). All points are the results of experiments with initial SIT of 1.5 m. The blue star and red star represent stations BS5 and NS2, respectively.

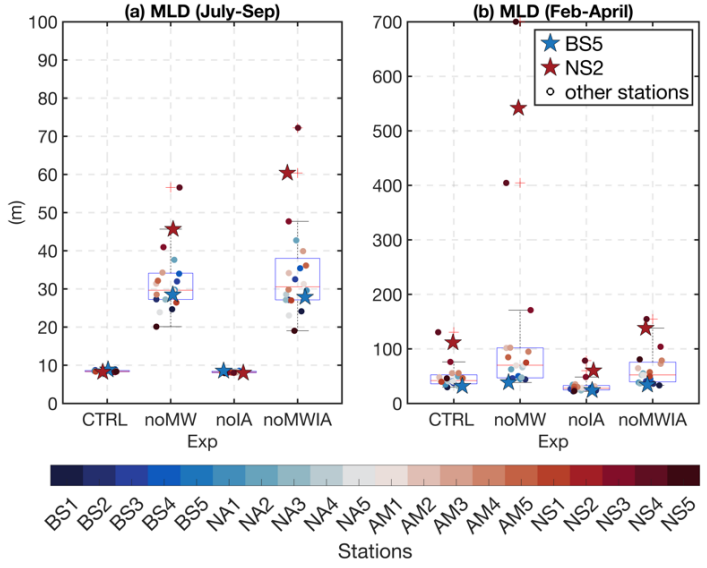

Figure S12. Box plots illustrating the mean (a) MLD in summer and (b) winter across different Stations in different types of experiments. Different stations are indicated by different colored dots. Each box plot shows the median, interquartile range, and potential outliers (points marked with red plus sign). All points are the results of experiments with initial SIT of 1.5 m. The blue star and red star represent stations BS5 and NS2, respectively.

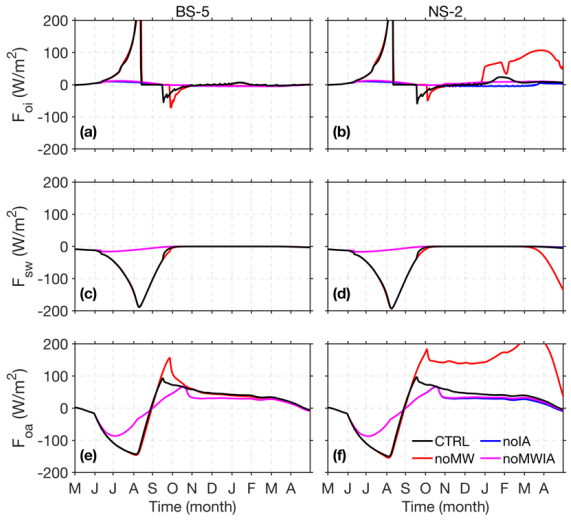

Figure S13. Time series of the heat flux at station BS5 (left column) and NS2 (right column). (a)-(b): F_{oi} (ocean-ice heat flux). (c)-(d): F_{sw} (solar shortwave flux). (e)-(f) F_{oa} (ocean-atmosphere heat flux) for the experiments with initial SIT of 1.5 m. Positive (negative) values denote upward (downward) heat flux, corresponding to oceanic heat loss (gain).

3 Diagnostic time series for NS2 station

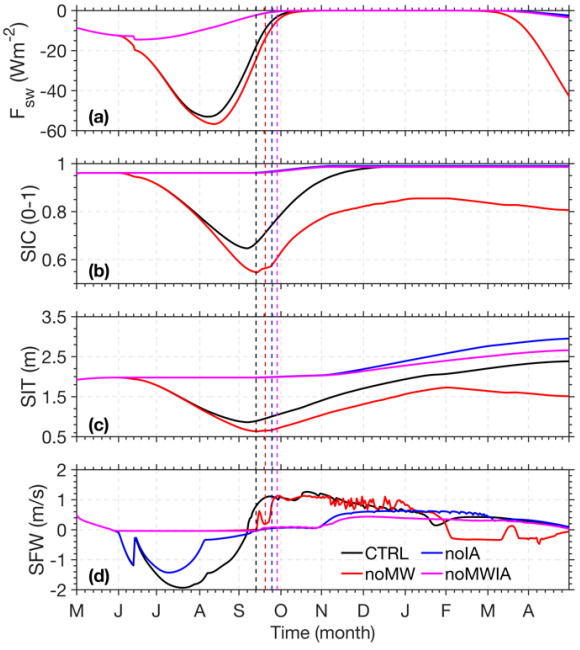

Figure S14. Figure 4. Modeled (a) net ocean shortwave heat flux, negative values represent heat entering the ocean. (b) ice concentration, (c) ice thickness and (d) net ocean surface freshwater flux at station NS2, negative values represent freshwater entering the ocean. The dashed lines perpendicular to the X-axis represent the first freezing day of each experiment (defined as the first day on which the ice thickness growth rate surpasses 0.1 cm/day).

4 Model results using climatological initial conditions

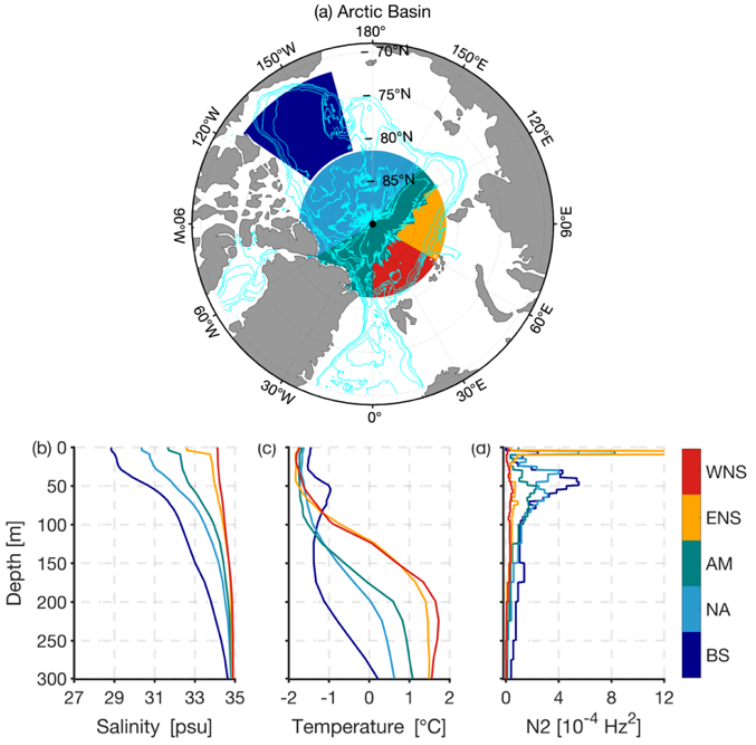

Figure S15. (a) Five sub-regions in the Arctic Ocean simulated using WOA2023 climatological data as the initial condition. BS: Beaufort Sea; NA: North of the Amerasian Basin; AM: Amundsen Basin; ENS: Eastern Nansen Basin; WNS: Western Nansen Basin. Corresponding profiles show (b) salinity, (c) temperature, and (d) buoyancy frequency.

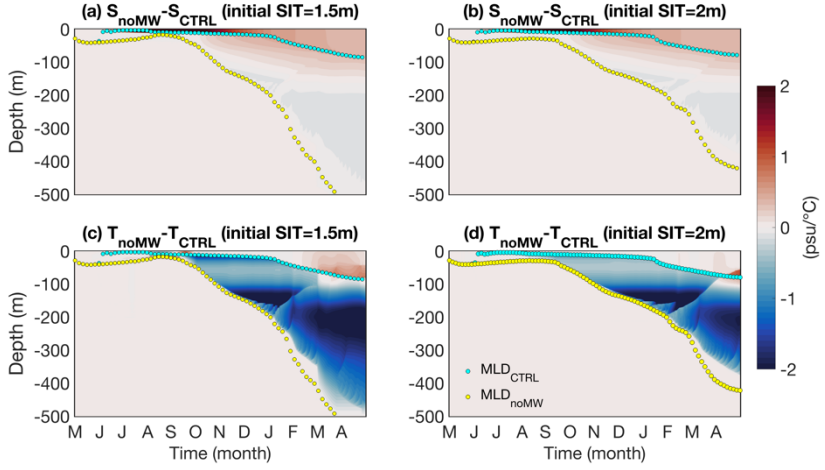

Figure S16. Modeled time series of ocean (a)-(b) salinity and (c)-(d) temperature differences in the WNS (noMW mins CTRL), using the WOA climatological data as the initial conditions. Left column: experiments with initial SIT of 1.5 m. Right column: experiments with initial SIT of 2 m. Colored dots indicate the MLD.

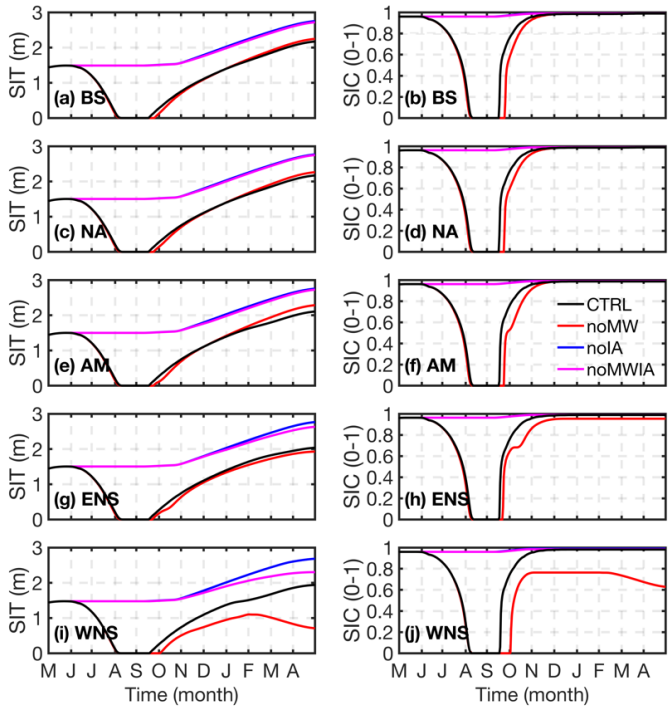

Figure S17. Modeled time development of SIT (left column) and SIC (right column) in all sub-regions, using WOA climatological data as the initial condition for experiments with initial SIT of 1.5 m.

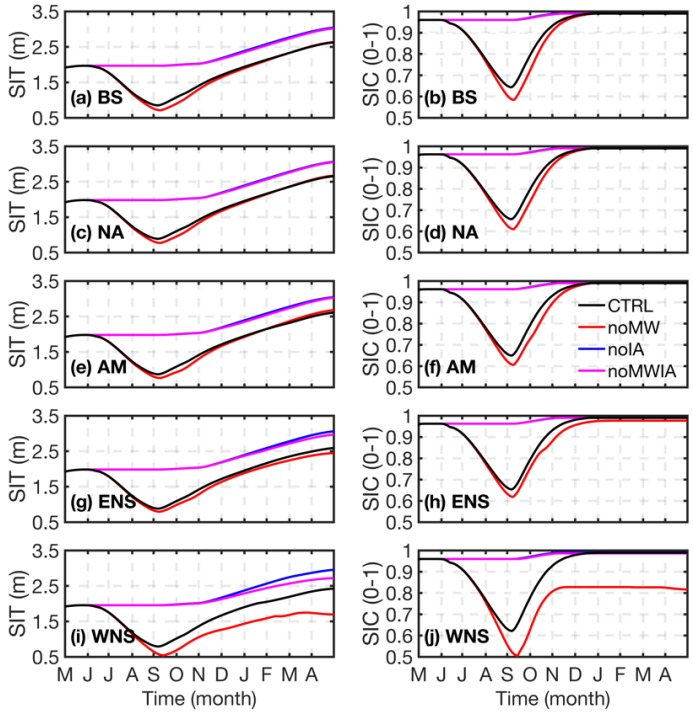

165 **Figure S18. Same as Figure S17 but for the experiments with initial SIT of 2 m.**

References

Carmack, E. C., Yamamoto-Kawai, M., Haine, T. W. N., Bacon, S., Bluhm, B. A., Lique, C., et al. (2016). Freshwater and its role in the Arctic Marine System: Sources, disposition, storage, export, and physical and biogeochemical consequences in the Arctic and global oceans. Journal of Geophysical Research: Biogeosciences, 121(3), 675–717. https://doi.org/10.1002/2015JG003140

Jackson, J. M., Carmack, E. C., McLaughlin, F. A., Allen, S. E., & Ingram, R. G. (2010). Identification, characterization, and change of the near-surface temperature maximum in the Canada Basin, 1993–2008. Journal of Geophysical Research: Oceans, 115(C5). https://doi.org/10.1029/2009JC005265

Krishfield, R. A., & Perovich, D. K. (2005). Spatial and temporal variability of oceanic heat flux to the Arctic ice pack. Journal of Geophysical Research, 110, C07021. https://doi.org/10.1029/2004JC002293

Landy, J. C., Dawson, G. J., Tsamados, M., Bushuk, M., Stroeve, J. C., Howell, S. E. L., et al. (2022). A year-round satellite sea-ice thickness record from CryoSat-2. Nature, 609(7927), 517–522. https://doi.org/10.1038/s41586-022-05058-5

Maykut, G. A., & McPhee, M. G. (1995). Solar heating of the Arctic mixed layer. Journal of Geophysical Research: Oceans, 100(C12), 24691–24703. https://doi.org/10.1029/95JC02554

McPhee, M. G., Kikuchi, T., Morison, J. H., & Stanton, T. P. (2003). Ocean-to-ice heat flux at the North Pole environmental observatory. Geophysical Research Letters, 30(24), 2274. https://doi.org/10.1029/2003GL018580

Peralta-Ferriz, C., & Woodgate, R. A. (2015). Seasonal and interannual variability of pan-Arctic surface mixed layer properties from 1979 to 2012 from hydrographic data, and the dominance of stratification for multiyear mixed layer depth shoaling. Progress in Oceanography, 134, 19–53. https://doi.org/10.1016/j.pocean.2014.12.005

Polyakov, I. V., Pnyushkov, A. V., Alkire, M. B., Ashik, I. M., Baumann, T. M., Carmack, E. C., et al. (2017). Greater role for Atlantic inflows on sea-ice loss in the Eurasian Basin of the Arctic Ocean. Science, 356(6335), 285–291. https://doi.org/10.1126/science.aai8204

Steele, M., Ermold, W., & Zhang, J. (2011). Modeling the formation and fate of the near-surface temperature maximum in the Canadian Basin of the Arctic Ocean. Journal of Geophysical Research: Oceans, 116(C11). https://doi.org/10.1029/2010JC006803

Zhong, W., Cole, S. T., Zhang, J., Lei, R., & Steele, M. (2022). Increasing winter ocean-to-ice heat flux in the Beaufort Gyre region, Arctic Ocean over 2006–2018. Geophysical Research Letters, 49, e2021GL096216. https://doi.org/10.1029/2021GL096216